Refinement indicators for estimating hydrogeologic parameters

M-H. Riahi, Hend Ben Ameur, Jérôme Jaffré, Rachida Bouhlila

Refinement indicators for estimating hydrogeologic parameters

Mohamed Hédi. Riahi[a,b], H.Ben Ameur[a,d] ,J. Jaffré[c] and R. Bouhlila [e]

a: ENIT-LAMSIN, University of Tunis El Manar, B.P. 37, Le Belvédère, 1002 Tunis, Tunisia;

b: ESPRIT 18, rue de l'Usine- ZI Aéport Charguia II 2035 Ariana, Tunisia;

c: INRIA Paris Rocquencourt, EPI SERENA, BP 105, 78153 Le Chesnay Cedex;

d: IPEST BP 51 2070 LA MARSA, Tunisia;

e: ENIT-LMHE, University of Tunis El Manar, B.P. 37, Le Belvédère, 1002 Tunis, Tunisia.

Abstract

We identify simultaneously the hydraulic transmissivity and the storage coefficient in a ground water flow governed by a linear parabolic equation. Both coefficients are assumed to be functions which are piecewise constant in space and constant in time. Therefore the unknowns are the coefficient values as well as the geometry of the zones where these parameters are constant. The identification problem is formulated as the minimization of a misfit least-square function. Using refinement indicators, we refine the parameterization locally and iteratively. We distinguish the cases where the two parameters have the same parameterization or different parameterizations.

keywords: Inverse problem, parameter estimation, parameterization, refinement indicators, storage coefficient, hydraulic transmissivity

1 Introduction

For most hydrogeological problems, such as management and protection of water resources, it is necessary to study flow and transfer of solutes in the subsurface. The corresponding mathematical models involve source terms, boundary and initial conditions and hydrological coefficients. Inverse modeling in groundwater applications provides ways of estimating these coefficients from a set of experimental measurements. This work is concerned with the presentation of an algorithm for solving the inverse problem of identifying hydrological coefficients, without using a priori information on the coefficients. The coefficients are assumed to be piecewise constant so we have to estimate not only their values but also the zones where the coefficients are constant. There may be one or several unknown coefficients.

Solving inverse problems in hydrogeology is well investigated [1, 2]. Some papers deal with source terms identification problems [3, 4, 5, 6]. A larger body of litterature is concerned, as we are in this paper, with the estimation of coefficients[7, 1, 8, 9, 10, 11, 12, 13]. Most often the proposed methods assume some sort of smoothness of the variation of these parameters. Alternatively, in this work, the considered situation is that of a zonation in which the coefficients vary smoothly inside the zones and jump heavily from one zone to the other. A first step in the inverse problem is then to identify the zones while assuming the coefficients to be constant in the zones, identifying actually the average values of the coefficient in each zone. In this paper we present an algorithm to do so. A second step would be to use more traditional methods inside each zone to take into account the variation of the coefficients inside each zone.

The assumption that parameters are constant on zones is already considered in [14, 15] but the set of zones (zonation) was determined by a priori information. The method proposed in this paper consists to build the parameterization in a progressive and iterative way without using a priori information on the parameters. The first iterative parameterization method is

the multiscale method [16, 17]. The drawback of this method, where the parameterization is uniformly refined during the iterations, is that it may lead to an overparameterization. The adaptive parameterization method proposed in [18] avoids this drawback since the refinement is local and depends on some "refinement indicator". This method was later used for a scalar parameter identification in [18, 19, 20, 21]. In [22], the parameterization method was extended to the identification of a vector parameter, the colour (Red Green Blue), in a problem of image segmentation. In such a problem the direct problem is actually the identity operator while in this paper it is a partial differential equation.

In this work, the adaptive parameterization method is guided by refinement indicators to identify simultaneously the storage coefficient and the hydraulic transmissivity in a confined aquifer which are both unknown. The two coefficients are assumed to be functions constant in time and since they are piecewise constant in space they present discontinuities at the interfaces between different geological zones where they are supposed to be constant. The unknowns of our inverse problem are the zonation and the values of the parameters in the zones. Different strategies are developed to deal with the cases where the two parameters have the same zonation or different zonations. The developed strategies can be used to identify more then two parameters.

Our inverse problem is formulated as a minimization problem of a least-squares function defined as a misfit between measurements and the corresponding quantities computed with "current" parameters. In order to ease the minimization procedure it is important to keep the number of unknowns in the minimization problem as small as possible. The data are measurements of the piezometric head in a confined aquifer which is the solution of a linear parabolic equation governing the flow.

The idea of the adaptive parameterization method is to refine a current parameterization according to refinement indicators. A refinement indicator indicates the effect on the optimal data misfit of adding some degree of freedom. The unknown parameterization is estimated, through an iterative process, by refining the scale at which the parameter distribution is described and the process is stopped when the refinement of the scale does not induce a significant decrease of the misfit function. An advantage of this method is to avoid overparameterization. At a given refinement level the parameter is estimated by minimizing the least-squares misfit function. Then refinement indicators are calculated and used to choose the next refinement level.

This paper is organized as follows. After the introduction in section 1, in section 2 the direct problem is introduced and the inverse problems is set as a minimization problem of a misfit function. Then the adjoint method for computing the gradient of that function is described. In section 3 the algorithm of adaptive parameterization is presented and different strategies are developed in order to construct parameterizations. Finally, in the fourth section several numerical experiments are presented corresponding to different versions of the parameterization algorithm for cases when the two parameters have the same zonation or as well as when they have two different zonations. The paper ends with concluding remarks.

2 Problem setting

Consider the following equations modeling groundwater flow in an isotropic and confined aquifer:

$$\begin{array}{lcll} S\dfrac{\partial \Phi}{\partial t} - \mathrm{div}(T\nabla\Phi) & = & Q & \text{in } \Omega \times (0,t_f) \\ \Phi & = & 0 & \text{on } \Gamma_D \times (0,t_f) \\ (-T\nabla\Phi)\cdot n & = & 0 & \text{on } \Gamma_N \times (0,t_f) \\ \Phi(0) & = & \Phi_0 & \text{in } \Omega \end{array} \tag{2.1}$$

where Ω is a bounded connected domain of $\mathbb{R}^2$, the time variable t belongs to the interval $(0,t_f)$, S is the storage coefficient and T is the hydraulic transmissivity, Φ is the piezometric head and Q is a distributed source terms. n is the outer normal to Ω, Γ_D and Γ_N are a partition of the boundary of Ω denoting respectively Dirichlet and Neumann conditions.

Equations (2.1) correspond to the direct problem where the unknown is Φ, all other variables, in particular, S and T, are known. We are interested in the inverse problem, where S and T are unknown and measurements of Φ are available. This inverse problem is formulated as a minimization problem of a least-square function $J(S,T)$, defined as a misfit between measurements of the piezometric head and the piezometric head computed with current parameters S and T:

$$J(S,T) = \frac{1}{2}\sum_{i=1}^{N_t}\sum_{j=1}^{m}(\Phi(t_i,M_j;S,T) - d_{ij}^{obs})^2 \tag{2.2}$$

where d_{ij}^{obs} is the piezometric head measured at time t_i and at point $M_j(x_j,y_j)$ and $\Phi(t_i,M_j;S,T)$ is the model output for the current coefficients S and T at the same time and the same point. Estimating the hydraulic transmissivity T and the storage coefficient S amounts to solving

$$\mathrm{Find}(S^*,T^*) = \underset{(S,T)\in U_{ad}}{\arg\min} \quad J(S,T) \tag{2.3}$$

where $U_{ad} = \{(S,T) : S_{min} \le S \le S_{max} \quad , \quad T_{min} \le T \le T_{max}\}$ is the set of admissible parameters.

Gradient methods are efficient methods for minimizing J. A crucial step in the minimization process is the computation of the gradient of the function J with respect to S and T. The adjoint method [23, 24, 1] provides an efficient way to compute this gradient and we present it here briefly. The weak formulation of the direct problem 2.1 is

$$\begin{array}{l} \text{Find } \Phi \in L^2(0,t_f;H_0^1(\Omega)) \cap C^0(0,t_f;L^2(\Omega)) \text{ as} \\ \displaystyle\int_\Omega S\partial_t\Phi v + \int_\Omega T\nabla\Phi\nabla v = \int_\Omega Qv \quad \forall v \in H_0^1(\Omega) \\ \Phi_{|t=0} = \Phi_0 \end{array} \tag{2.4}$$

where $L^2(0,t_f;H_0^1(\Omega))$ is the space of square-integrable functions on $(0,t_f)$ with values in $H_0^1(\Omega)$ and $C^0(0,t_f;L^2(\Omega))$ is the space of continuous functions on $(0,t_f)$ with values in $L^2(\Omega)$.

To minimize J under the constraint (2.1) we introduce the Lagrangien $\mathcal{L}$:

$$\mathcal{L}(S,T;\Phi,\Phi^*) = J(S,T) + \int_0^{t_f}\int_\Omega S\partial_t\Phi\Phi^* dt + \int_0^{t_f}\int_\Omega T\nabla\Phi\nabla\Phi^* dt - \int_0^{t_f}\int_\Omega Q\Phi^* dt. \tag{2.5}$$

Note that if $\Phi(S,T)$ satisfies (2.4) then Equation (2.5) becomes

$$\mathcal{L}(S,T;\Phi,\Phi^*) = J(S,T) \quad \forall\Phi^* \in H_0^1(\Omega). \tag{2.6}$$

From Equation (2.6) it follows

$$\frac{\partial J}{\partial T}\delta T + \frac{\partial J}{\partial S}\delta S = \frac{\partial \mathcal{L}}{\partial \Phi}\delta\Phi + \frac{\partial \mathcal{L}}{\partial \Phi^*}\delta\Phi^* + \frac{\partial \mathcal{L}}{\partial T}\delta T + \frac{\partial \mathcal{L}}{\partial S}\delta S. \tag{2.7}$$

We choose $\Phi^* \in H_0^1(\Omega)$ such that

$$\frac{\partial \mathcal{L}}{\partial \Phi}(\Phi(S,T),\Phi^*;S,T)\delta\Phi = 0 \quad \forall\delta\Phi \in H_0^1(\Omega). \tag{2.8}$$

This choice leads to a simplification of Equation (2.7). Φ^* is the adjoint state and Equation (2.8) is the adjoint equation which we can rewrite as

$$\begin{array}{lcll} -S\dfrac{\partial\Phi^*}{\partial t} - div(T\nabla\Phi^*) & = & \displaystyle\sum_{i=1}^{N_t}\sum_{j=1}^{m}(\Phi(t_i,M_j;S,T) - d_{ij}^{obs})\delta(t-t_i)\delta(x-x_j) & \\ & & & \text{in } \Omega\times(0,t_f), \\ \Phi^* & = & 0, & \text{on } \Gamma_D\times(0,t_f), \\ (-T\nabla\Phi^*)\cdot n & = & 0, & \text{on } \Gamma_N\times(0,t_f), \\ \Phi^*(t_f) & = & 0, & \text{in } \Omega \end{array} \tag{2.9}$$

where $\delta(.)$ is the Dirac δ-function.
Taking into account Equations (2.7), (2.8) the gradient of J can be written as

$$\begin{array}{rcl} \dfrac{\partial J}{\partial T}\delta T + \dfrac{\partial J}{\partial S}\delta S & = & \dfrac{\partial \mathcal{L}(S,T;\Phi,\Phi^*)}{\partial T}\delta T + \dfrac{\partial \mathcal{L}(S,T;\Phi,\Phi^*)}{\partial S}(H,p;S,T)\delta S \\ & = & \displaystyle\int_0^{t_f}\int_\Omega \delta T\nabla\Phi\nabla\Phi^* \quad d\Omega dt + \int_0^{t_f}\int_\Omega \delta S\frac{\partial\Phi}{\partial t}\Phi^* \quad d\Omega dt. \end{array} \tag{2.10}$$

It follows that

$$\frac{\partial J}{\partial T} = \int_0^{t_f}\int_\Omega \nabla\Phi\nabla\Phi^* d\Omega dt, \quad \frac{\partial J}{\partial S} = \int_0^{t_f}\int_\Omega \frac{\partial\Phi}{\partial t}\Phi^* d\Omega dt. \tag{2.11}$$

Equations (2.1) and (2.9) are discretized using the finite element method in space. For the numerical resolution of the direct equations (2.1) and the adjoint equations (2.9), the software SUTRA [25] was used. The minimization of the misfit function J is obtained by the code N2QN1 [26]. This optimizer implements a quasi-Newton (BFGS) method with line search.

3 Parameterization

The choice of a parameterization is a crucial point in for a successful parameter estimation. As we chose piecewise constant representation of the coefficients, for each coefficient and at each iteration we build a zonation which is a partition of the domain into zones where the coefficient is constant. Then the value of the coefficient in each zone is calculated. The proposed method will produce an optimal parameterization, in the sense that it minimizes the number of zones, and consequently the number of unknowns necessary to explain the available data. The zonations can be viewed as discretization grids for the coefficients. If we had used the computational mesh for the coefficient discretization, the inverse problem would have a very large number of unknowns resulting in an optimization problem of very large dimension. There would not be any balance between the amount of data and the number of unknowns and we would not be able to obtain meaningful results.

The idea of adaptive parameterization method is to refine the zonation iteratively by adding at each iteration only one degree of freedom obtained by dividing one zone of the current zonation into two zones The choice of the zone to be refined and the choice of the refining cut are given by the refinement indicators. The new zone is added where the refinement indicators indicate that it should induce a significant decrease of the misfit function. So the refinement of the parametrization is not arbitrary and not uniform. In this work we suppose that interfaces between zones are carried by the edges of the computational mesh. The refining cuts are thus carried by the edges of mesh cells and belong to a predefined set of curves.

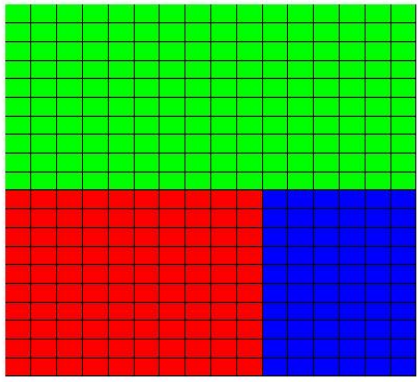

Figure 3.1: Parametrization (colored zones) and computation mesh (fine grid).

3.1 Refinement indicators

In this section, following [18], we recall what is a refinement indicator and how it allows to select the refinement which is likely to induce the largest decrease of the misfit function. Let us consider an example where the initial zonation includes only one rectangular zone Z_0 (see figure 3.2) and we will proceed to its refinement by cutting it into two rectangular zones $Z_{1,1}$ and $Z_{1,2}$.

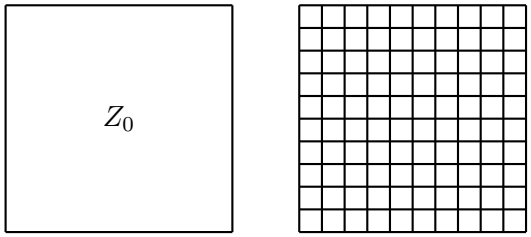

Figure 3.2: Initial zonation (on the left) and computing mesh (on the right)

Let us suppose that the vectorial parameter is constant in the hole domain $\Omega = Z_0$, and denote by m_0 this parameter. In our case $m_0 = \begin{pmatrix} S_0 \\ T_0 \end{pmatrix}$, where T_0 is the hydraulic transmissivity and S_0 is the the storage coefficient. The optimization problem (2.3) corresponding to this one-zone parameterization $\mathcal{Z}_0$ is

$$m_0^{opt} = \arg \min_{m_0 \in U_{ad}} J_{\mathcal{Z}_0}(m_0). \tag{3.1}$$

Now the goal is to refine the zonation into a zonation with two zones with the aim to decrease the misfit function. Each component S and T of the vectorial parameter m may have its own zonation: $\mathcal{Z}_{S1}$, $\mathcal{Z}_{T1}$. Let us divide Z_0 into two rectangular zones $Z_{S1,1}$ et $Z_{S1,2}$ for the component S and two others $Z_{T1,1}$ et $Z_{T1,2}$ for the component T, $Z_0 = Z_{S1,1} \cup Z_{S1,2} = Z_{T1,1} \cup Z_{T1,2}$. New zones are separated by the cuts C_{S1} and C_{T1}. The new zonations are $\mathcal{Z}_{S1} = \{Z_{S1,i}\}_{i=1,2}$ and $\mathcal{Z}_{T1} = \{Z_{T1,i}\}_{i=1,2}$. Denote by $\mathcal{Z}_1 = \{\mathcal{Z}_{S1}, \mathcal{Z}_{T1}\}$. The unknown of the optimization problem (2.3) corresponding to the refined zonation is $m_1 = (S_{1,1}, S_{1,2}, T_{1,1}, T_{1,2})^t$. Denote by

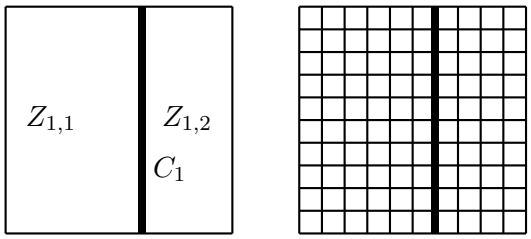

Figure 3.3: Left: a two-zone zonation $\mathcal{Z}_{S1}$ for the coefficient. Right: computational mesh for solving the direct and adjoint problems. The vertical cut C_1 is marked with a bold line.

$c = \begin{pmatrix} c_S \\ c_T \end{pmatrix}$ the discontinuities of S and T respectively across C_{S1} and C_{T1} :

$$c_S = S_{1,1} - S_{1,2}, \quad c_T = T_{1,1} - T_{1,2}.$$

Introducing the matrix $A = \begin{pmatrix} 1 & -1 & 0 & 0 \\ 0 & 0 & 1 & -1 \end{pmatrix}$ and assuming that c is known the estimation of $m1$ comes to solve an optimization problem under the constraint $Am_1 = c$

$$m_1^{opt} = \arg \min_{Am_1 = c} J_{\mathcal{Z}_1}(m_1) \tag{3.2}$$

where $J_{\mathcal{Z}_1}$ is the misfit function corresponding to the new zonation $\mathcal{Z}_1$. Note that the minimisation problem (3.1) is equivalent to (3.2) when $c = 0$.

To the minimization under constraint problem (3.2) let us associate the Lagrangian function

$$L_{\mathcal{Z}_1}(m_1, \lambda) = J_{\mathcal{Z}_1}(m_1) + \left\langle \lambda_{\mathcal{Z}_1}, Am_1 - c \right\rangle \tag{3.3}$$

where $\lambda_{\mathcal{Z}_1} = \begin{pmatrix} \lambda_{S,\mathcal{Z}_1} \\ \lambda_{T,\mathcal{Z}_1} \end{pmatrix}$ is the Lagrange mutiplier associeted to the contraint $Am_1 = c$. The optimality conditions associated to (3.2) are then :

$$\begin{array}{rcccl} \dfrac{\partial L_{\mathcal{Z}_1}(m_1^{opt}, \lambda_{\mathcal{Z}_1}^{opt})}{\partial m_1} & = & \nabla J_{\mathcal{Z}_1}(m_1^{opt}) + A^t \lambda_{\mathcal{Z}_1}^{opt} & = & 0, \\ \dfrac{\partial L_{\mathcal{Z}_1}(m_1^{opt}, \lambda_{\mathcal{Z}_1}^{opt})}{\partial \lambda} & = & Am_1^{opt} - \lambda_{\mathcal{Z}_1}^{opt} & = & 0. \end{array} \tag{3.4}$$

Taking into account the optimality conditions (3.4) and deriving the Lagrangian function $L_{\mathcal{Z}_1}$ with respect to c, we obtain

$$\frac{\partial L_{\mathcal{Z}_1}(m_1^{opt}, \lambda_{\mathcal{Z}_1}^{opt})}{\partial c}\Big|_{c=0} = \frac{\partial L_{\mathcal{Z}_1}(m_1^{opt}, \lambda_{\mathcal{Z}_1}^{opt})}{\partial m_1}\Big|_{c=0} \frac{\partial m_1}{\partial c} + \frac{\partial L_{\mathcal{Z}_1}(m_1^{opt}, \lambda_{\mathcal{Z}_1}^{opt})}{\partial \lambda}\Big|_{c=0} \frac{\partial \lambda}{\partial c} = 0$$

Using (3.3) it follows that

$$\frac{\partial L_{\mathcal{Z}_1}(m_1^{opt}, \lambda_{\mathcal{Z}_1}^{opt})}{\partial c}\Big|_{c=0} = \nabla_c J_{\mathcal{Z}_1}(m_1^{opt})\Big|_{c=0} - \lambda_{\mathcal{Z}_1}^{opt} = 0,$$

and

$$\lambda_{\mathcal{Z}_1}^{opt} = \nabla_c J_{\mathcal{Z}_1}(m_1^{opt})\Big|_{c=0}. \tag{3.5}$$

The Taylor expansion of $J_{\mathcal{Z}_1}$ as a function of the discontinuity c in a neighborhood of $c = 0$ is

$$J_{\mathcal{Z}_1}(m_1^{opt})\Big|_c = J_{\mathcal{Z}_1}(m_1^{opt})\Big|_{c=0} + \left\langle c, \nabla_c J_{\mathcal{Z}_1}(m_1^{opt})\Big|_{c=0} \right\rangle + o(||c||).$$

Since $J_{\mathcal{Z}_1}(m_1^{opt})\Big|_{c=0} = J_0(m_0^{opt})$ we conclude that $\left\langle c, \nabla_c J_{\mathcal{Z}_1}(m_1^{opt})\Big|_{c=0} \right\rangle = \left\langle c, \lambda_{\mathcal{Z}_1}^{opt} \right\rangle$ models at a first order the variation between $J_{\mathcal{Z}_1}(m_1^{opt})$ and $J_{\mathcal{Z}_0}(m_0^{opt})$ in a neighborhood of $c = 0$. Without solving the optimization problem (3.2) computing $\lambda_{\mathcal{Z}_1}^{opt}$ allows to conclude if the zonation refinement induced by the cuts C_{S1} and C_{T1} would produce a significant decrease of the misfit function or not.

The components of $\lambda_{\mathcal{Z}_1}^{opt}$ give two refinement indicators $I_S^{\mathcal{Z}_1}, I_T^{\mathcal{Z}_1}$ corresponding respectively to the cuts C_{S1} and C_{T1} inducing the zonation $\mathcal{Z}_1$.
Note that the refinement indicator is calculated with the gradient of $J_{\mathcal{Z}_1}$ with respect to the values of the coefficients in the zones. This gradient can be easily calculated from "the fine gradient" computed on the computing mesh:

$$\frac{\partial J_{\mathcal{Z}_1}}{\partial S_{1,i}}(m_1^{opt}) = \sum_{K \subset Z_{S1,i}} \frac{\partial J_{\mathcal{Z}_1}}{\partial S_K}(m_1^{opt}), \quad \frac{\partial J_{\mathcal{Z}_1}}{\partial T_{1,i}}(m_1^{opt}) = \sum_{K \subset Z_{T1,i}} \frac{\partial J_{\mathcal{Z}_1}}{\partial T_K}(m_1^{opt}),\ i = 1, 2 \tag{3.6}$$

where K denotes a cell of the computing mesh. Thus using the adjoint method (see Section 2) is crucial for an efficient computation of the gradient and of the refinement indicators.

In this work, to refine a zone by dividing it into two zones, only vertical and horizontal cuts carried by the computational mesh edges are used (other cuts are possible, see [18]).

3.2 Algorithm

We are adapting an algorithm initially proposed in [18] for the estimation of a scalar parameter in porous media and extended in [22] to image segmentation with a vector parameter whose components are the three colors $Red, Green, Blue$. In image segmentation the direct problem is just the identity model, while for the hydrogeological problem, the model is given by (2.1) which require the solution of a PDE. Therefore the application of the adaptive parameterization algorithm is more complex.

We choose an initial zonation $\mathcal{Z}_0 = \Omega$. A step of the algorithm is as follows:

1. Given a zonation $\mathcal{Z}_{k-1} = (\mathcal{Z}_{S,k-1}, \mathcal{Z}_{T,k-1})$ with k zones for each parameter, minimize $J_{\mathcal{Z}_{k-1}}$ to obtain an optimal parameter m_k^{opt}.

2. Build a new zonation $\widetilde{\mathcal{Z}}_k = (\widetilde{\mathcal{Z}}_{S,k}, \widetilde{\mathcal{Z}}_{T,k})$ with $k+1$ zones for each parameter, by introducing a cut dividing a zone into two zones following four steps:

   (a) Consider $\mathcal{C}^{ad}$ the set of cuts C giving a possible zonation $\widetilde{\mathcal{Z}}_k^C$ having $k+1$ zones for each parameter obtained by dividing into two zones only one zone in $\mathcal{Z}_{S,k-1}$ and only one zone in $\mathcal{Z}_{T,k-1}$.

   (b) For each $C \in \mathcal{C}^{ad}$ we compute $\lambda^{opt}_{\widetilde{\mathcal{Z}}_k^C} = (\lambda^{opt}_{S,\widetilde{\mathcal{Z}}_k^C}, \lambda^{opt}_{T,\widetilde{\mathcal{Z}}_k^C})$ using (3.5), (3.6).

   (c) For each zone $\widetilde{\mathcal{Z}}_k^C$, $C \in \mathcal{C}^{ad}$, compute a refinement indicator $\widetilde{I}_k^C$ from vectors $\lambda^{opt}_{\widetilde{\mathcal{Z}}_k^C}$ according to a choosen strategy proposed in the following Section 3.3.

   (d) Select a set of zonations $\widetilde{\mathcal{Z}}_k^C$, $C \in \mathcal{C}_k \subset \mathcal{C}^{ad}$ corresponding to the largest values of $\widetilde{I}_k^C$ and for each of these zonations minimize $J_{\widetilde{\mathcal{Z}}_k}$.

3. Update the zonation by taking fo each $\mathcal{Z}_k$ the zonation $\widetilde{\mathcal{Z}}_k^C$ which produces the largest decrease of the misfit function.

The stopping criteria for the algorithm are:

- The value of the misfit function is close to zero.
- The misfit function stops decreasing during a number of iterations.
- The values of the refinement indicators are small.
- The norm of the gradient of the misfit function is small.

3.3 Strategies for the computation of the refinement indicators

In this section, inspired by [22], we develop different strategies for the computation of refinement indicators $\widetilde{I}_k^C$ from the Lagrange mutiplier $\lambda^{opt}_{\widetilde{\mathcal{Z}}_k^C}$ computed in (3.6).

3.3.1 Strategy 1: Euclidean norm for refinement indicators

In this strategy we assume that the two coefficients S and T have the same zonation, we define the refinement indicators by

$$\widetilde{I}_k^C = \sqrt{\left(\lambda^{opt}_{S,\widetilde{\mathcal{Z}}_k^C}\right)^2 + \left(\lambda^{opt}_{T,\widetilde{\mathcal{Z}}_k^C}\right)^2}.$$

Since the refinement indicator is a scalar the adaptive parametrization algorithm can be applied as in the scalar case described in [18]. At each iteration we perform the following steps:

1. Compute $I_k^{max} = \max_{C \in \mathcal{C}^{ad}} \widetilde{I}_k^C$.
2. Introduce the subset of cuts $\mathcal{C}_\delta^{ad} = \{C \in \mathcal{C}^{ad} : \widetilde{I}_k^C \geq \delta * I_k^{max}\}$ to $0.5 \leq \delta \leq 1$.
3. Minimize the misfit function for each partition corresponding to a cut $C \in \mathcal{C}_\delta^{ad}$.
4. Keep only the cut C^* which induces the largest decrease of the misfit function.

This strategy is efficient if both parameters S and T have the same zonation.

3.3.2 Strategy 2: Best cut for all parameters

In this strategy the algorithm is guided by two refinement indicators, one for each coefficient S and T. Two sets of possible cuts are selected according to the two indicators. During an iteration, a temporary selection is made with respect to only one of the two parameters. At the end of the iteration the same cut is applied to both parameters. It is chosen according to the criterion of "best decrease" of the misfit function. At each iteration the first steps are as follows:

1. Compute the refinement indicators: $I_{S,k}^{max} = \max_{C \in \mathcal{C}_S^{ad}} \lambda_{S,\widetilde{\mathcal{Z}}_k^C}^{opt}, I_{T,k}^{max} = \max_{C \in \mathcal{C}_T^{ad}} \lambda_{T,\widetilde{\mathcal{Z}}_k^C}^{opt}$.
2. Introduce the subset of cuts $\mathcal{C}_{S\delta}^{ad} = \{C \in \mathcal{C}_S^{ad} : \widetilde{I}_{S,k}^C \geq \delta * I_{S,k}^{max}\}$ to $0.5 \leq \delta \leq 1$.
3. Introduce the subset of cuts $\mathcal{C}_{T\delta}^{ad} = \{C \in \mathcal{C}_T^{ad} : \widetilde{I}_{T,k}^C \geq \delta * I_{T,k}^{max}\}$ to $0.5 \leq \delta \leq 1$.
4. Minimize the misfit function freezing the zonation for T at $\mathcal{Z}_{T,k-1}$ and using as zonation for S, the zonations $\widetilde{\mathcal{Z}}_{S,k}^C$ where $C \in \mathcal{C}_S^{ad}$. Keep only the cut C_S^* that maximizes the decrease of the misfit function.
5. Minimize the misfit function by freezing the zonation for S at $\mathcal{Z}_{S,k-1}$ and using as zonation for T, the zonations $\widetilde{\mathcal{Z}}_{T,k}^C$ where $C \in \mathcal{C}_T^{ad}$. Keep only the cut C_T^* that maximizes the decrease of the misfit function.

Then, after obtaining a cut for each parameter, we apply the following steps:

1. Minimize the misfit function with the zonation obtained by applying the cut C_S^* for both parameters S and T.
2. Minimize the misfit function with the zonation obtained by applying the cut C_T^* for both parameters S and T.
3. Keep for the two parameters the cut $C^* = C_S^*$ or C_T^* which induces the largest decrease of the misfit function.

Thus, going from one iteration to the next, we introduce the same cut for S and T.

3.3.3 Strategy 3: Best cut for each parameter

In this strategy, parameters S and T are treated independently. The choice of this strategy is justified by the case where the geological zones for the storage coefficient and the transmissivity are different. The zonations are constructed by applying steps (1), (2) and (3) of the previous subsection followed by:

(4) Minimize the misfit function by freezing the zonation for T at $\mathcal{Z}_{T,k-1}$ and use as zonation for S, the zonation $\widetilde{\mathcal{Z}}^{C}_{S,k}$ for $C \in \mathcal{C}^{ad}_{S}$. Keep only the cut C^*_S that maximizes the decrease of the misfit function.

(5) Minimize the misfit function by freezing the zonation for S at $\mathcal{Z}_{S,k-1}$ and use as zonation for T, the zonation $\widetilde{\mathcal{Z}}^{C}_{T,k}$ for $C \in \mathcal{C}^{ad}_{T}$. Keep only the cut C^*_T that maximizes the decrease of the misfit function.

(6) The new zonation is $\mathcal{Z}_k = (\widetilde{\mathcal{Z}}^{C^*_S}_{S,k}, \widetilde{\mathcal{Z}}^{C^*_T}_{T,k})$.

4 Numerical experiments

Consider as an example the aquifer of Rocky Mountain Arsenal, Denver, Colorado in USA [25] represented in Figure 4.1. This aquifer is horizontal and rectangular. The computational

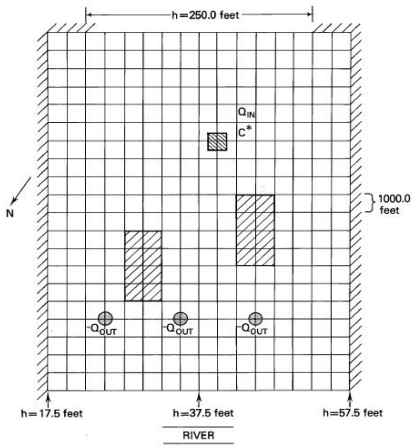

Figure 4.1: Geometry of the Rocky Mountain aquifer.

domain is discretized with a mesh of 320 square elements and 357 nodes, while the time interval is 10 days and a time step is 2 days. The thickness of the aquifer is equal to $40ft$. In this aquifer, there are four wells, three pumping wells with a constant rate $Q_{out} = -0.2ft^{-3}/s$ and an injection well with a constant rate $Q_{IN} = 10ft^{-3}/s$ (see Figure 4.1). The lateral boundaries are impermeable. On the top boundary, the piezometric head is set constant and equal to $250.0ft$. On the bottom boundary, the piezometric head is varying linearly from left to right from $17.5ft$ to $57,5ft$. The exact hydraulic transmissivity and storage coefficient are constant in the whole aquifer with values $T = 2.5\ 10^{-4}m/s$, $S = 6.00\ 10^{-7}$, except in inclusions where their values are $T = 2.5\ 10^{-6}m/s, S = 9.95\ 10^{-7}$.

In the following two situations are considered. In the first situation the two exact coefficients are those described in the Rocky Mountain Arsenal aquifer and they share the same

zonation with two inclusions as shown in Figure 4.2. In a second situation we constructed a model where each coefficient has its own inclusion as in Figure 4.3, their respective values being the same as in the first situation. The mesh represented in Figures 4.2, Figure 4.3 is that of the numerical discretization of the computational domain.

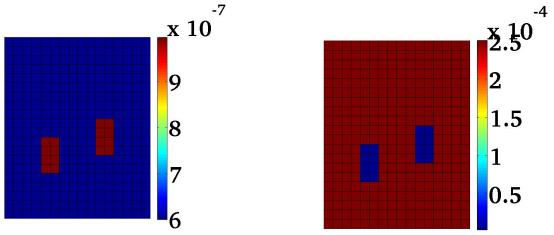

Figure 4.2: Exact coefficients S (left) and T (right) with the same zonation.

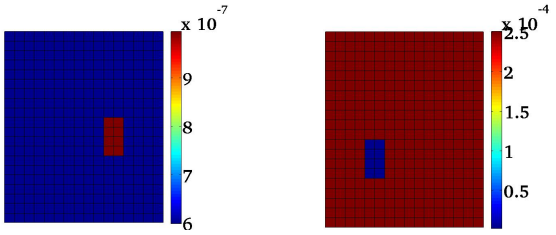

Figure 4.3: Exact coefficients S (left) and T (right) with different zonations.

In a first series of experiments the data are measurements of the piezometric head at each node of the computing mesh and at each time step. In a second series of experiments the number of measurements will be reduced. These measurements will be the observations of the numerical solution calculated with the exact coefficients.

Figure 4.4 shows the piezometric head computed with the exact coefficients which is used as data d^{obs}. We observe two depressions corresponding to the two inclusions with very low permeability compared to the surrounding domain and we notice a peak located at the injection well.

The purpose of this section is to compare the performances of the three different strategies presented in section 3.3 for computing the refinement indicators. In all experiments the initial guess for the coefficients is a constant throughout the whole domain.

4.1 Experiments using the euclidean norm for refinement indicators (strategy 1)

In Test 1 the exact coefficients S and T have the same zonation as in Figure 4.2.

To identify the zonation of the coefficients S and T and their values in each zone, we use the algorithm described in section 3.2 with strategy 1, where the refinement indicator is defined as the euclidean norm of the vector indicator $I = (I_S, I_T)$. In the initial parameterization the two coefficients S and T are constant in the whole domain and their initial values are $(S_0, T_0) = (6.00\ 10^{-7}, 2.5\ 10^{-4})$. Applying strategy 1 the zonation is the same for both

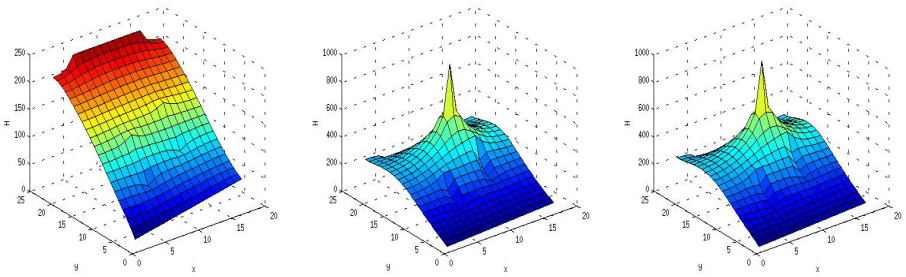

Initial time After 6 days Final time

Figure 4.4: Test 1: piezometric head at 3 times calculated with the coefficients shown in Figure 4.2.

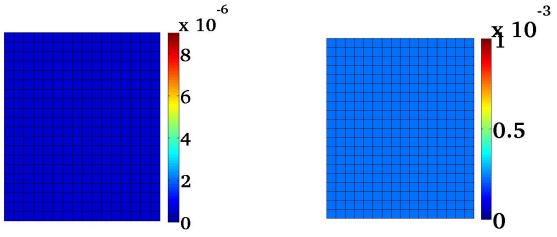

Figure 4.5: Test 1: optimal values of S (left) and T (right) after the first minimization.

coefficients at all iterations. Going from one iteration to the next, the current zonation for the two coefficients is refined by introducing one cut corresponding to the largest decrease of the misfit function.

Figure 4.6 shows the evolution of the coefficient values during the iterations of the algorithm. It should be noted that colors correspond to coefficient values and do not represent the zones. If a coefficient has the same value in two different adjacent zones these zones have the same color but a change of color corresponds to a change of zone.

We remark that in the third iteration edges limiting a large zone sourrounding the two inclusions that we are looking for are already identified. At the 9th iteration, both sought inclusions start to appear and they are identified at iteration 14. The exact parameter values are obtained at the 16th iteration. Note that the exact T is obtained faster than the storage coefficient. This behavior will be observed in all experiments and is due to a smaller sensitivity of the system to S than to T. Figure 4.7 shows the final zonation with 16 zones and the variation of the normalized misfit function during the iterations.

In Test 2 the same strategy is applied to a case where the exact coefficients have the same values as in Test 1 but with different zonations as in Figure 4.3. Figure 4.8 shows the values of the coefficients obtained during the iterations.

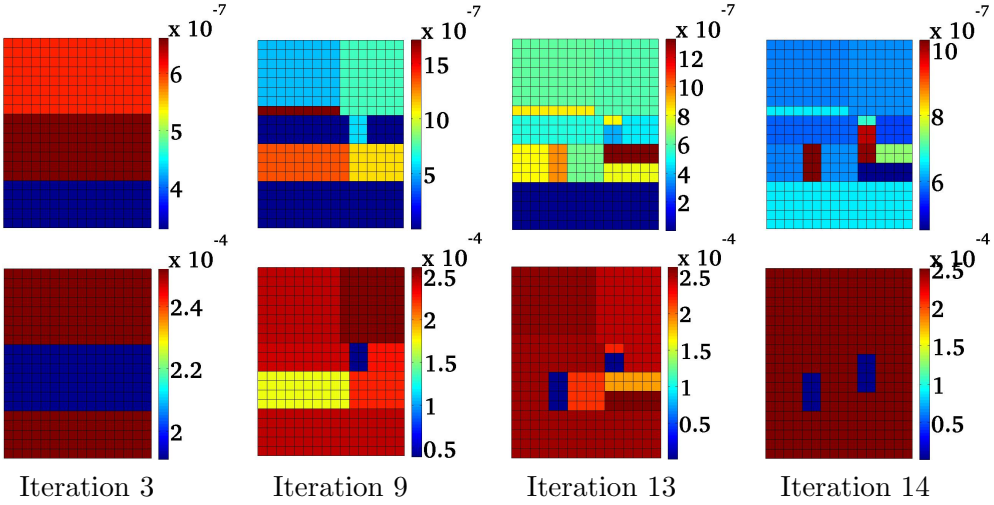

Figure 4.6: Test 1: coefficients S (top row) and T (bottom row) computed during the iterations with strategy 1, when exact S and T have the same zonation.

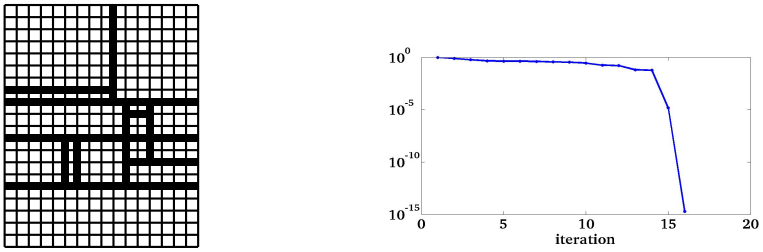

Figure 4.7: Test 1: strategy 1 when exact S and T have the same zonation. Final zonation for S and T and variation of the misfit function during the iterations with strategy 1.

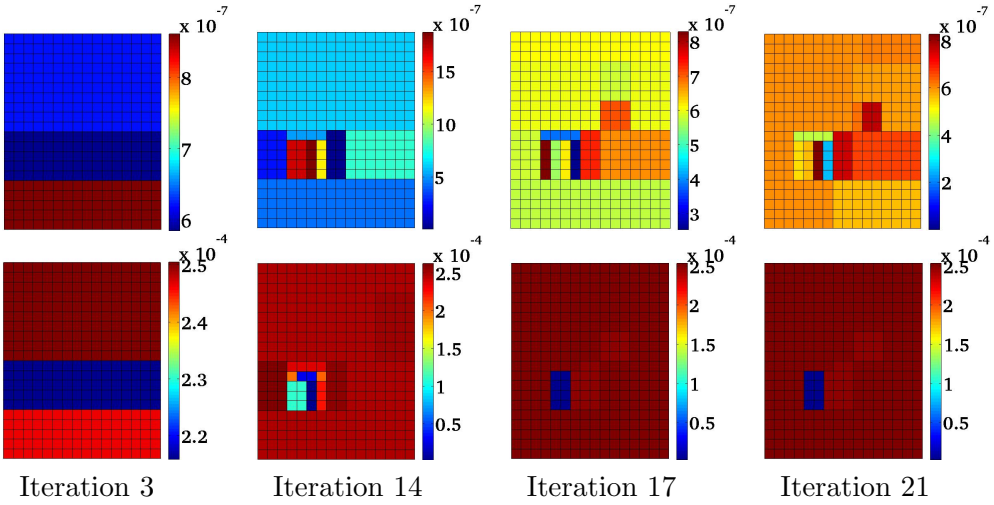

Figure 4.8: Test 2: coefficients S (top row) and T (bottom row) computed during the iterations with strategy 1, when exact S and T have different zonations.

The algorithm identifies T at iteration 17, but then fails to identify S. Figure 4.9 shows the final zonation for the two coefficients after 20 iterations and the variation of the normalized misfit function during the iterations.

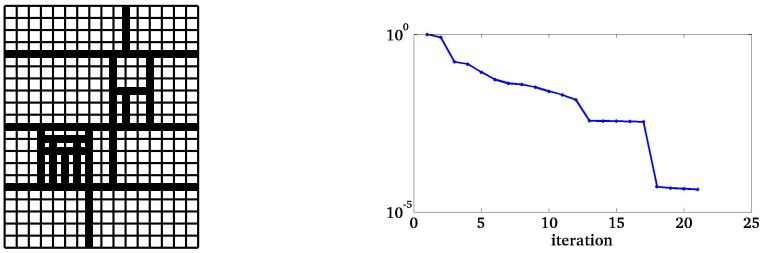

Figure 4.9: Test 2: strategy 1 when exact S and T have different zonations. Zonation after 21 iterations (left) and variation of the misfit function during the iterations (right).

4.2 Experiments using the best cut for the two coefficients (strategy 2)

Strategy 2 is now applied using the same data as in Tests 1 and 2: going from one iteration to the next, we add the same cut for both coefficients corresponding to the largest decrease of the misfit function. Again strategy 2 calculates the same zonation for both coefficients.

Test 3 corresponds to the case where the two exact coefficients have the same zonation (Figure 4.2) and Test 4 corresponds to the case where the two exact coefficients have different zonations (Figure 4.3). Initialization is the same as before.

Figure 4.10 gives the evolution of the computed coefficients during the iterations. It took 24 iterations to obtain the exact coefficients, a few more iterations than in Test 1. Again T was identified first. Figure 4.11 shows the final zonation obtained after 24 iterations and the variation of the normalized misfit function during the iterations.

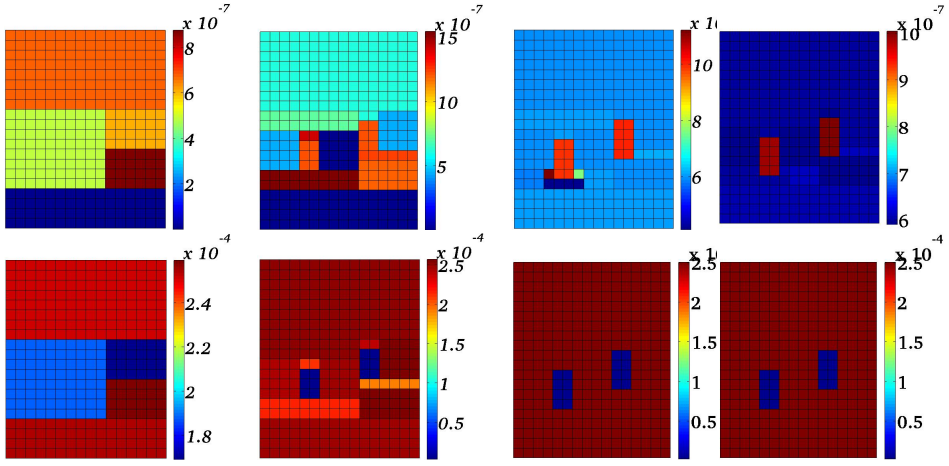

Figure 4.10: Test 3: coefficients S (top row) and T (bottom row) computed at iteration 24 using strategy 2, when exact S and T have the same zonation.

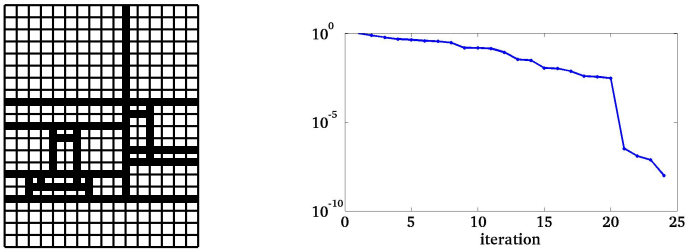

Figure 4.11: Test 3: zonation after 24 iterations for the two coefficients and variation of the misfit function during the iterations.

Strategy 2 is now applied to the case where the two coefficients have different zonations. The algorithm is initialized as before. Figure 4.12 shows the variation of the computed coefficients during the iterations. At iteration 10 the zonation and the exact values of the hydraulic transmissivity are identified. For the storage coefficient, more iterations are needed to find its zonation and its values. This is due to the weak sensitivity of the system to this coefficient.

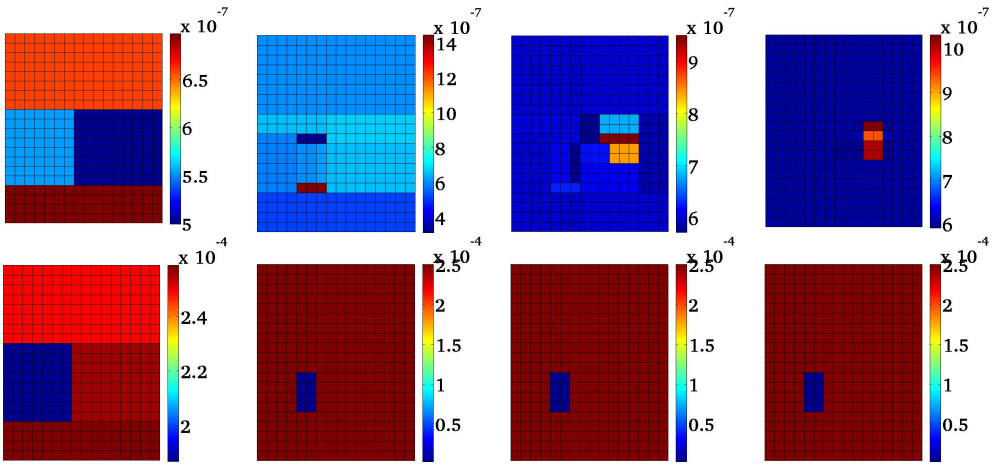

Figure 4.12: Test 4: coefficients S (top row) and T (bottom row) computed during the iterations using strategy 2, when exact S and T have different zonations.

Figure 4.13 shows the zonation for the two calculated coefficients and the variation of the normalized misfit function during the iterations.

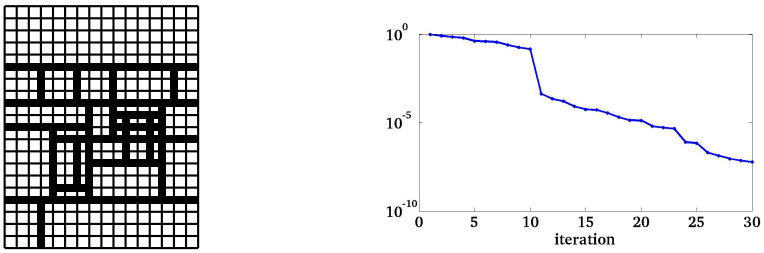

Figure 4.13: Test 4: strategy 2 when the two exact coefficients have different zonations. Zonation for S and T after 29 iterations (left) and variation of the misfit function during the iterations (right).

4.3 Experiments using the best cut for each parameter (strategy 3)

The main feature of this strategy is that during the algorithm iterations the two coefficients are treated independently. Each coefficient has its own zonation constructed with its own refinement indicator as described in section 3.3.3. For the case where the two coefficients have the same zonation Figure 4.14 shows the variation of the computed coefficients during the iterations. The algorithm identifies T after 24 iterations but fails to identify S.

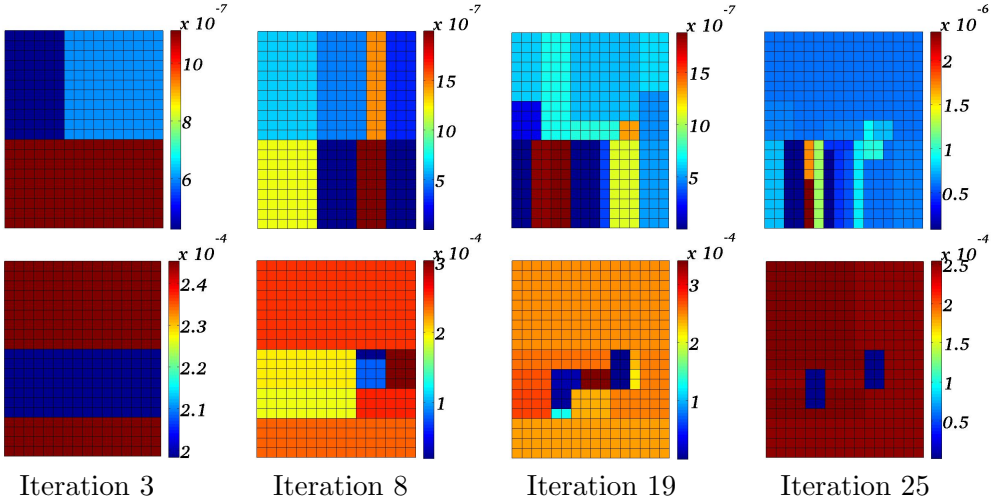

Figure 4.14: Test 5: coefficients S (top row) and T (bottom row) computed during the iterations using strategy 3, when exact S and T have the same zonation.

Figure 4.15 shows zonations for S and T after 28 iterations and the variation of the normalized misfit function during the iterations.

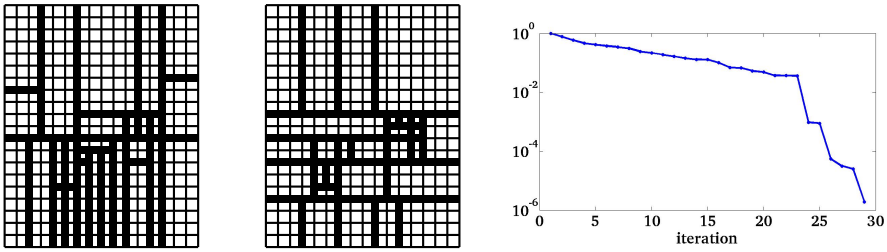

Figure 4.15: Test 5: strategy 3 when the two exact coefficients have the same zonation. Zonations for S and T after 28 iterations (left and center) and variation of the misfit function during the iterations (right).

Strategy 3 is now applied to the case where the exact coefficients have different zonations (see Figure 4.3). As before, the algorithm is initialized with a single zone for each coefficient. Figure 4.16 shows the variation of the computed coefficients during the iterations. Figure 4.14 shows the variation of the computed coefficients during the iterations. Figure 4.17 shows zonations for S and T after 12 iterations and the variation of the normalized misfit function during the iterations. The algorithm identifies S and T after 12 iterations.

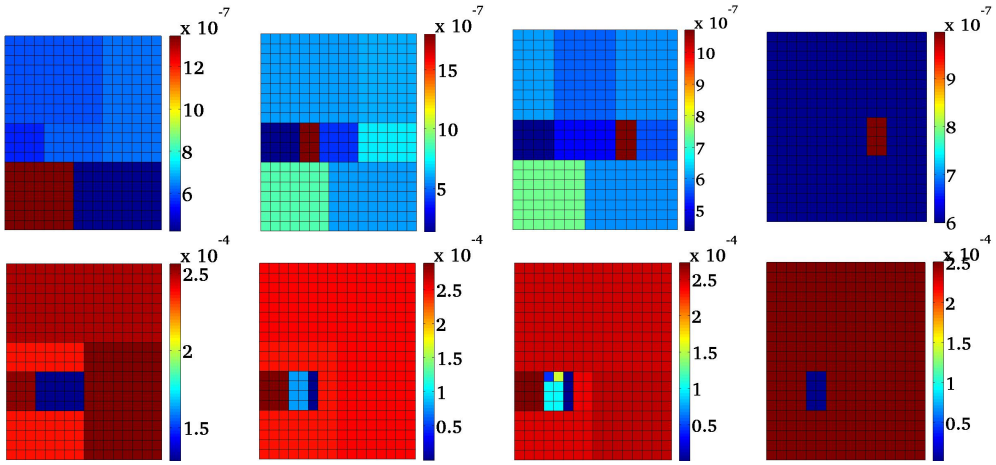

Figure 4.16: Test 6: coefficients S (top row) and T (bottom row) computed during the iterations using strategy 3, when exact S and T have different zonations.

4.4 Summary of results

Results for convergence for different strategies and different exact zonations are summarized in Table 1. They show that strategy 1 works well when both exact coefficients have the same zonation while strategy 3 works well when the two coefficients have different zonations. Strategy 2 works well in both cases.

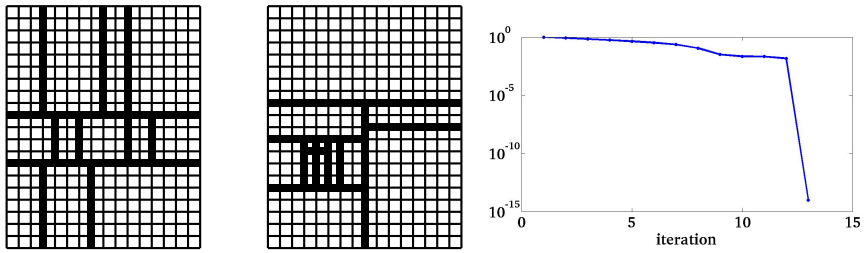

Figure 4.17: Test 6: strategy 3 when the two exact coefficients have different zonations. Zonations for S and T after 12 iterations (left and center) and variation of the misfit function during the iterations (right).

	Strategy 1		Strategy 2		Strategy 3	
	S	T	S	T	S	T
Same exact zonation for S and T	16	14	24	20	fails	25
Different exact zonations for S and T	fails	21	29	10	12	12

Table 1: Number of iterations for convergence of S and T for different strategies and different exact zonations.

In all cases the smaller sensitivity of the system to S than to T is observed by the higher number of iterations for convergence for S than for T, and even in some instances the failure to converge for S while the algorithm was converging for T.

4.5 Influence of the number of measurements

The number of measurements is now decreased. Considering the two cases where the parameters have the same or different zonations, for each case the more efficient strategy is applied, that is strategy 1 for the first case and strategy 3 for the second case. For each of these cases three tests are investigated corresponding to different locations of the observation points shown in Figure 4.18: in a first test there is one observation point out of 2 cells, in a second test there is one observation point out of four cells and in the third test there is 17 observation points distributed randomly. The time sampling of data is not changed. In order to evaluate the fit to the data achieved by the algorithm with different number of observation points, we introduce the percentage of explained data

$$1 - \sqrt{\frac{\sum_{i,j} |\Phi(t_i, M_j; S, T) - d_{ij}^{obs}|^2}{\sum_{i,j} |d_{ij}^{obs}|^2}}.$$

Case of strategy 1 with exact coefficients having the same zonation (Fig. 4.2)

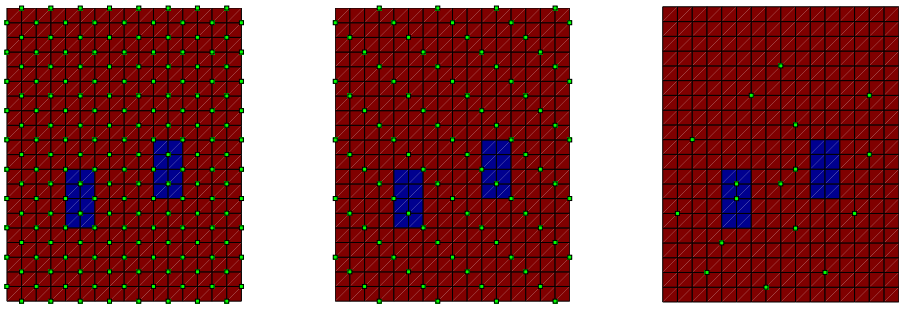

Figure 4.18: Points of observations: every other point (left), one point out of four(middle), random (right). The inclusions are colored in blue.

Three tests are performed by changing the number of measurement points and the location of these points. Test 7 uses one observation point out of 2 cells (Figure 4.18 left), Test 8 uses one observation point out of 4 cells (Figure 4.18 middle) and Test 9 uses the a random distribution of observation points (Figure 4.18 right). The results obtained for these two experiments are summarized in Table 2. Figure 4.19 and Figure 4.20 show only for Tests 8 and 9 the values of the obtained coefficients and the decrease of the misfit function during the iterations. The corresponding figures are not shown for Test 7 since the coefficients were recovered almost exactly.

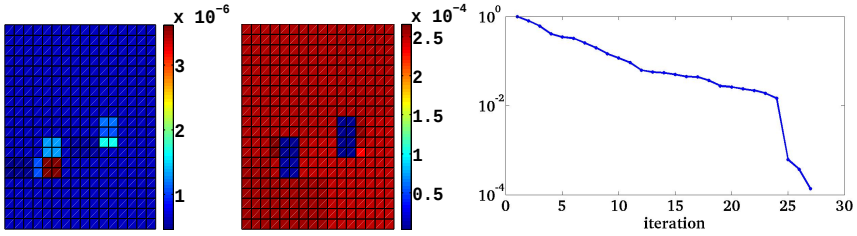

Figure 4.19: Test 8: strategy 1, when exact S and T have the same zonation. Coefficients S (left) and T (center) computed after 24 iterations and variation of the misfit function (right). Observation points as in Figure 4.18 middle.

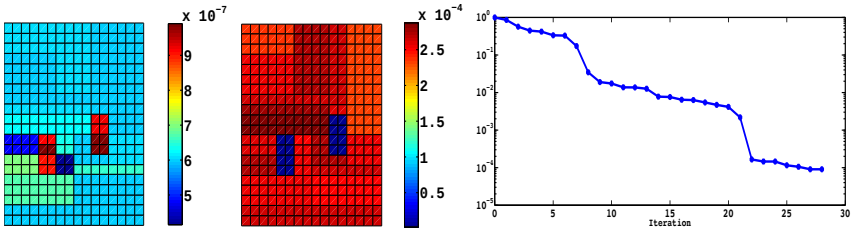

Figure 4.20: Test 9: strategy 1, when exact S and T have the same zonation. Coefficients S (left) and T (center) computed after 26 iterations and variation of the misfit function (right). Observation points as in Figure 4.18 right.

One can observe that the algorithm did well at identifying the zonation shared by S and

Observation points	1 out of 2 vertices	1 out of 4 vertices	random
Final # of iterations	24	26	28
Final # of zones	24	26	28
J^{opt}	$9.31\ 10^{-6}$	$1.37\ 10^{-4}$	$9.045\ 10^{-5}$
% of explained data	0.99	0.96	0.94

Table 2: Results with a reduced number of measurements, strategy 1 and case of exact coefficients with the same zonation

T, even with a small number of observation points.

Case of strategy 3 with exact coefficients having different zonations (Fig. 4.3)

The experiments performed previously with strategy 1 when the coefficients share the same zonation are now run again with strategy 3 when the zonations for each coefficient are different. Test 10 uses one observation point out of 2 cells (Figure 4.18 left), Test 11 uses one observation point out of 4 cells (Figure 4.18 middle) and Test 12 uses the a random distribution of observation points (Figure 4.18 right). Figures 4.21 and 4.22 show for Tests 11 and 12 the values of the obtained coefficients and the decrease of the misfit function during the iterations. Results are summarized in Table 3. In Figures 4.21 and 4.22 one can observe that the dark brown color for the inclusion for S and the dark blue color for the inclusion for T are clearly isolated which show that the algorithm identified the zonations of each coefficient, even with a small number of observation points.

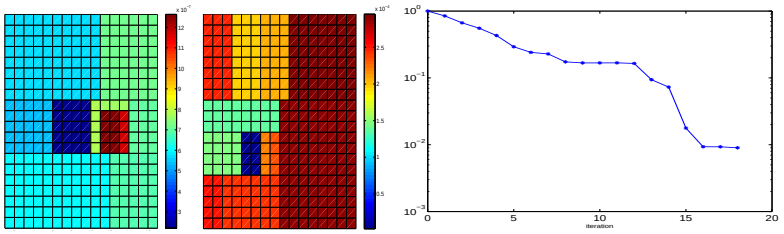

Figure 4.21: Test 11: strategy 3, when exact S and T have different zonations. Coefficients S (left) and T (center) computed after 18 iterations and variation of the misfit function (right). Observation points as in Figure 4.18 middle.

Observation points	1 out of 2 vertices	1 out of 4 vertices	random
Final # of iterations	14	18	20
Final # of zones	14	18	20
J^{opt}	$7.13\ 10^{-4}$	$9.54\ 10^{-3}$	$2.94\ 10^{-5}$
% of explained data	0.97	0.94	0.93

Table 3: Results with a reduced number of measurements, strategy 3 when exact S and T have different zonations.

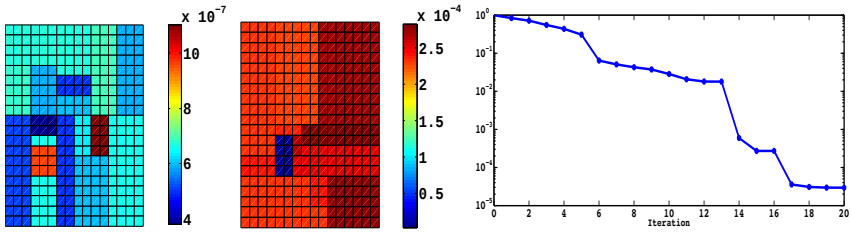

Figure 4.22: Test 12: strategy 3, when exact S and T have different zonations. Coefficients S (left) and T (center) computed after 20 iterations and variation of the misfit function (right). Observation points as in Figure 4.18 right.

References

[1] Sun NZ. Inverse problems in groundwater modeling. Kluwer Academic Publishers; 1994.

[2] OM Alifanov SR EA Artyukhin. Extreme methods for solving ill-posed problems with applications to inverse heat transfer problems. Begell house New York; 1995.

[3] Atmadja J, Bagtzoglou AC. State of the art report on mathematical methods for groundwater pollution source identification. Environmental forensics. 2001;2(3):205–214.

[4] Huang CH, Li JX, Kim S. An inverse problem in estimating the strength of contaminant source for groundwater systems. Applied mathematical modelling. 2008;32(4):417–431.

[5] Kriksin YA, Plushchev S, Samarskaya EA, Tishkin VF. The inverse problem of source reconstruction for convective diffusion equation. Matematicheskoe Modelirovanie. 1995; 7(11):95–108.

[6] Nguyen VT, Nguyen HT, Tran TB, Vo AK. On an inverse problem in the parabolic equation arising from groundwater pollution problem. Boundary Value Problems. 2015; 2015(1):67.

[7] Yeh WWG. Review of parameter identification procedures in groundwater hydrology: The inverse problem. Water Resources Research. 1986;22(2):95–108.

[8] De Marsily G, Buoro A, et al. 40 years of inverse problems in hydrogeology. Comptes Rendus de l'Academie des Sciences Series IIA Earth and Planetary Science. 1999;329(2):73–87.

[9] Carrera J, Medina A, Galarza G. Groundwater inverse problem: Discussion on geostatistical formulations and validation. Hydrogeologie. 1993;4:313–324.

[10] Kitanidis PK, Vomvoris EG. A geostatistical approach to the inverse problem in groundwater modeling (steady state) and one-dimensional simulations. Water resources research. 1983;19(3):677–690.

[11] Kuiper LK. A comparison of several methods for the solution of the inverse problem in two-dimensional steady state groundwater flow modeling. Water Resources Research. 1986;22(5):705–714.

[12] McLaughlin D. Investigation of alternative procedures for estimating ground-water basin parameters. 1975;.

[13] McLaughlin D, Townley LR. A reassessment of the groundwater inverse problem. Water Resources Research. 1996;32(5):1131–1161.

[14] Cooley RL. Incorporation of prior information on parameters into nonlinear regression groundwater flow models: 1. theory. Water Resources Research. 1982;13:318–324.

[15] Cooley RL. Incorporation of prior information on parameters into nonlinear regression groundwater flow models: 2. applications. Water Resources Research. 1983;19:662–676.

[16] Chavent G, Liu J. Multiscale parametrization for the estimation of a diffusion coefficient in elliptic and parabolic problems. In: Jai AE, Amouroux M, editors. 5th IFAC Symposium on Control of Distributed Parameter Systems, Perpignan; 1989 June 26–29; France. Université de Perpignan, France; 1997. p. 315–324.

[17] Liu J. A multiresolution method for distributed parameter estimation. SIAM Journal on Scientific Computing. 1993;14(2):389–405.

[18] BenAmeur H, Chavent G, Jaffré J. Refinement and coarsening indicators for adaptive parametrization: application to the estimation of hydraulic transmissivities. Inverse Problems. 2001;18(3):775.

[19] Grimstad A, Mannseth T, Nævdal G, Urkedal H. Adaptive multiscale permeability estimation. Computational Geosciences. 2003;7:1–25.

[20] Hayek M, Ackerer P. An adaptive subdivision algorithm for the identification of the diffusion coefficient in two-dimensional elliptic problems. Journal of Mathematical Modelling and Algorithms. 2007;6(4):529–545.

[21] Hayek M, Ackerer P, Sonnendrücker É. A new refinement indicator for adaptive parameterization: Application to the estimation of the diffusion coefficient in an elliptic problem. Journal of Computational and Applied Mathematics. 2009;224(1):307–319.

[22] BenAmeur H, Clément F, Weis P, Chavent G. The multidimensional refinement indicators algorithm for optimal parameterization. Journal of Inverse and Ill-Posed Problems. 2008;16:107–126.

[23] Chavent G. On the theory and practice of non-linear least-squares. Advances in Water Resources. 1991;14(2):55–63.

[24] Chavent G. Nonlinear least squres for inverse problems: Theoretical foundations and step-by=step guide for applications. Springer; 2009.

[25] Voss CI. A finite-element simulation model for saturated-unsaturated, fluid-density-dependent ground-water flow with energy transport or chemically-reactive single-species solute transport. Vol. 84. US Geological Survey; 1984.

[26] Bonnans F, Gilbert JC, Lemaréchal C, Sagastizábal C. Optimisation numérique: aspects théoriques et pratiques. 1997;.